Geodesic Discrete Global Grid Systems

Kevin Sahr, Denis White, and A. Jon Kimerling

ABSTRACT: In recent years, a number of data structures for global geo-referenced data sets have been proposed based on regular, multi-resolution partitions of polyhedra. We present a survey of the most promising of such systems, which we call Geodesic Discrete Global Grid Systems (Geodesic DGGSs). We show that Geodesic DGGS alternatives can be constructed by specifying five substantially independent design choices: a base regular polyhedron, a fixed orientation of the base regular polyhedron relative to the Earth, a hierarchical spatial partitioning method defined symmetrically on a face (or set of faces) of the base regular polyhedron, a method for transforming that planar partition to the corresponding spherical/ellipsoidal surface, and a method for assigning point representations to grid cells. The majority of systems surveyed are based on the icosahedron, use an aperture 4 triangle or hexagon partition, and are either created directly on the surface of the sphere or by using an equal-area transformation. An examination of the design choice options leads us to the construction of the Icosahedral Snyder Equal Area aperture 3 Hexagon (ISEA3H) Geodesic DGGS.

KEYWORDS: Discrete global grid systems, spatial data structures, global data models

Discrete Global Grid Systems: Basic Definitions

Discrete Global Grid

A Discrete Global Grid (DGG) consists of a set of regions that form a partition of the Earth's surface, where each region has a single point contained in the region associated with it. Each region/point combination is a *cell*. Depending on the application, data objects or vectors of values may be associated with regions, points, or cells. If an application defines only the regions, the centroids of the regions form a suitable set of associated points. Conversely, if an application defines only the points, the Voronoi regions of those points form an obvious set of associated cell regions.

Applications often use DGGs with cell regions that are irregular in shape and/or size. For example, the division of the Earth's surface into land masses and bodies of water constitutes one of the most important DGGs. A more general example, the Hipparchus System (Lukatella 2002), allows the creation of arbitrarily regular DGGs by generating Voronoi cells on the surface of an ellipsoid from a specified set of points. But, for many applications, it is desirable to have cells consisting of highly regular regions with evenly distributed points.

Regular DGGs are unbiased with respect to spatial patterns created by natural and human processes and allow for the development of simple and efficient algorithms. A single regular DGG may play multiple data structure roles. It may function as a raster data structure, where each cell region constitutes a pixel. It may serve as a vector data structure, where the set of DGG points replaces traditional coordinate pairs (Dutton 1999). Each data object may be associated with the smallest cell region in which it is fully contained, and these minimum bounding cells may then be used as a coarse filter in operations such as object intersection. The DGG can also be used as a useful graph data structure by taking the DGG points as the graph vertices and then connecting points associated with neighboring cells with unit-weight edges.

The most commonly used regular DGGs are those based on the geographic (latitude–longitude) coordinate system. Raster global data sets often employ cell regions with edges defined by arcs of equal-angle increments of latitude and longitude (for example, the 2.5^0 x 2.5^0, 5^0 x 5^0, and 10^0 x 10^0 NASA Earth Radiation Budget Experiment (ERBE) grids described in Brooks (1981)). Data values may also be associated with points spaced at equal-angle intervals of latitude and longitude (for example, the 5' x 5' spacing of the ETOPO5 global elevation data set

Kevin Sahr is an Assistant Professor in the Department of Computer Science at Southern Oregon University, Ashland, OR 97520. E-mail: <ksahr@earthlink.net>. **Denis White** is a Geographer at the US EPA NHEERL Western Ecology Division, Corvallis, OR 97333. E-mail: <white.denis@epa.gov>. **A. Jon Kimerling** is a Professor in the Department of Geosciences at Oregon State University, Corvallis, OR 97331. E-mail: <kimerlia@geo.orst.edu>.

(Hastings and Dunbar 1998)). Similarly, vector data sets that employ a geographic coordinate system to define location values commonly choose a specific precision for those values. The choice of a specific precision for geographic coordinates forms an implicit grid of fixed points at regular angular increments of latitude and longitude, and a particular data set of that precision can consist only of coordinate values chosen from this set of fixed points. Ideally, the regions associated with the geographic vector coordinate points would be the corresponding Voronoi regions on the Earth's surface, although they are more commonly the corresponding Voronoi regions on a surrogate representation of the Earth's surface, such as a sphere or ellipsoid. In practice, applications often implicitly employ Voronoi regions defined on the longitude x latitude plane, on which the regions are, conveniently, regular planar squares. As we shall see, employing a surrogate representation for the Earth's surface on which the cell regions are regular planar polygons is a useful and common approach in DGG construction.

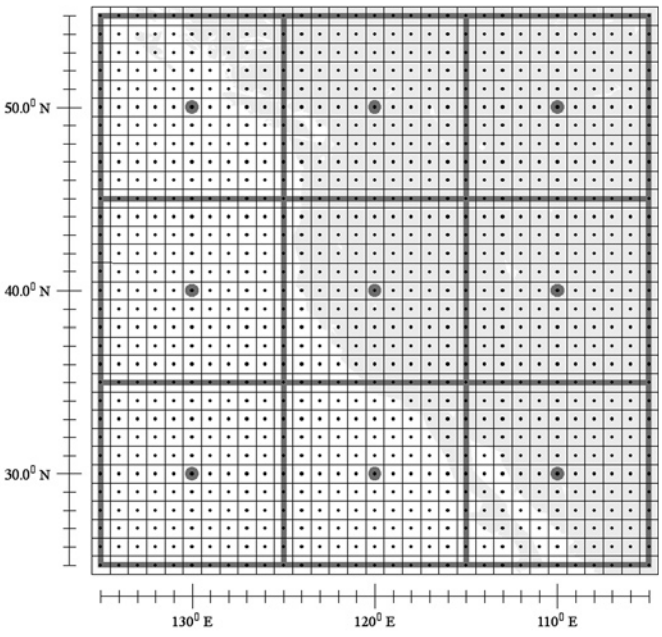

Figure 1. A portion of two resolutions (10^0 and 1^0 precision) of the DGGS implicitly generated by multiple precisions of decimal geographic coordinate system vector representations. Note that this is an incongruent, aligned hierarchy.

Discrete Global Grid System

A Discrete Global Grid System (DGGS) is a series of discrete global grids. Usually, this series consists of increasingly finer resolution grids; i.e., the grids in the series have a monotonically increasing number of cells. If the grids are defined consistently using regular planar polygons on a surrogate surface, we can define the *aperture* of a DGGS as the ratio of the areas of a planar polygon cell at resolution k and at resolution $k+1$ (this is a generalization of the definition given in Bell et al.(1983)). Later we will discuss DGGSs that have more than one type of polygonal cell region. In these cases there is always one cell type that clearly predominates, and the aperture of the system is defined using the dominant cell type.

Kimerling et al. (1999) and Clarke (2002) note the importance of regular hierarchical relationships between DGGS resolutions in creating efficient data structures. Two types of hierarchical relationship are common. A DGGS is *congruent* if and only if each resolution k cell region consists of a union of resolution $k+1$ cell regions. A DGGS is *aligned* if and only if each resolution k cell point is also a cell point in resolution $k+1$. If a DGGS does not have these properties, the system is defined as *incongruent* or *unaligned*. For example, the most widely used DGGS is generated implicitly by multiple precisions of decimal geographic vector representations. This DGGS has an aperture of 10 and is incongruent and aligned (Figure 1).

Discrete Global Grid Systems based on the geographic coordinate system have numerous practical advantages. The geographic coordinate system has been used extensively since well before the computer era and is therefore the basis for a wide array of existing data sets, processing algorithms, and software. Grids based on square partitions are by far the most familiar to users, and they map efficiently to common data structures and display devices.

But such grids also have limitations. Discrete Global Grid Systems induced by the latitude–longitude graticule do not have equal-area cell regions, which complicates statistical analysis on these grids. The cells become increasingly distorted in area, shape, and inter-point spacing as one moves north and south from the equator. The north and south poles, both points on the surface of the globe, map to lines on the longitude x latitude plane; the top and bottom row of grid cells are, in fact, triangles, not squares as they appear on the plane. These polar singularities have forced applications such as global climate modeling to make use of special grids for the polar regions. Square grids in general do not exhibit uniform adjacency; that is, each square grid cell has four neighbors with which it shares an edge and whose centers are equidistant from its center. Each cell, however, also has four neighbors with which it shares only a vertex and whose centers are a different distance from its center than the distance to the centers of the edge neighbors. This compli-

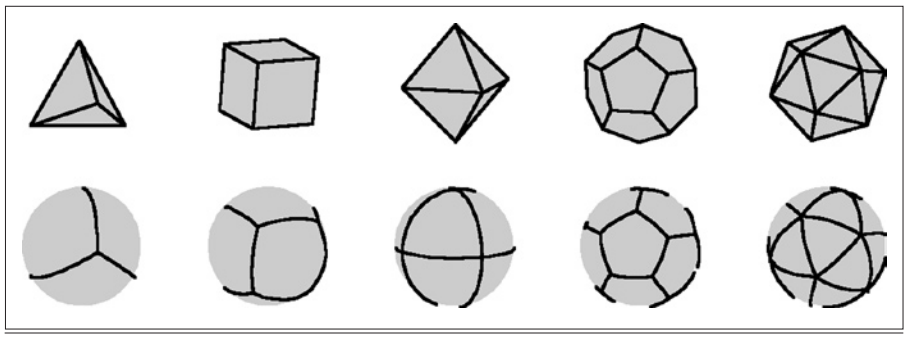

Figure 2. Planar and spherical versions of the five platonic solids: the tetrahedron, hexahedron (cube), octahedron, dodecahedron, and icosahedron.

cates the use of these grids for such applications as discrete simulations.

Attempts have been made to create DGGs based on the geographic coordinate system but adjusted to address some of these difficulties. For example, Kurihara (1965) decreased the number of cells with increasing latitude so as to achieve more consistent cell region sizes. Bailey (1956), Paul (1973), and Brooks (1981) used similar adjustments of latitude and/or longitude cell edges to achieve cell regions with approximately equal areas. But these schemes achieved more regular cell region areas at the cost of more irregular cell region shapes and more complex cell adjacencies. Tobler and Chen (1986) projected the Earth onto a rectangle using a Lambert cylindrical equal area projection and then recursively subdivided that rectangle, but, as in the case of the other mentioned approaches, this did not address the basic problem that the sphere/ellipsoid and the plane are not topologically equivalent.

Geodesic Discrete Global Grid Systems

The inadequacies of DGGSs based on the geographic coordinate system have led a number of researchers to explore alternative approaches. Many of these approaches involve the use of regular polyhedra as topologically equivalent surrogates for the Earth's surface, and, in our opinion, these attempts have led to the most promising known options for DGGSs. A number of researchers have been inspired directly or indirectly by R. Buckminster Fuller's work in discretizing the sphere, which led to his development of the geodesic dome (Fuller 1975). We will thus refer to this class of DGGSs as Geodesic Discrete Global Grid Systems.

Geodesic DGGSs have been proposed for a number of specific applications. Inherently regular in design, these systems have most commonly been used to store raster data sets, but they may also be used as a substitute for traditional coordinate-based vector data structures (Dutton 1999), as data containers, or as the basis for graphs (as described in the previous section). Geodesic DGGSs have been used to develop statistically sound survey sampling designs on the Earth's surface (Olsen et al. 1998), for optimum path determination (Stefanakis and Kavouras 1995), for line simplification (Dutton 1999), for indexing geospatial databases (Otoo and Zhu 1993; Dutton 1999; Alborzi and Samet 2000), and for the generation of spherical Voronoi diagrams (Chen et al. 2003). They have also been proposed as the basis for dynamic simulations such as those used in global climate modeling (Williamson 1968; Sadournay et al. 1968; Heikes and Randall 1995a, 1995b; Thuburn 1997).

It is highly unlikely that any single Geodesic DGGS will ever prove optimal for all applications. Many of the proposed systems include design innovations in particular areas, though their construction may have involved other, less desirable design choices. Therefore, rather than surveying individual Geodesic DGGSs as monolithic, closed systems, we will take the approach here of viewing the construction of a Geodesic DGGS as a series of design choices which are, for the most part, independent. The following five design choices fully specify a Geodesic DGGS:

1. A base regular polyhedron;
2. A fixed orientation of the base regular polyhedron relative to the Earth;
3. A hierarchical spatial partitioning method defined symmetrically on a face (or set of faces) of the base regular polyhedron;
4. A method for transforming that planar partition to the corresponding spherical/ellipsoidal surface; and
5. A method for assigning points to grid cells.

We will now look at each of these design choices in turn, discussing the decisions made in the development of a number of Geodesic DGGSs.

Base Regular Polyhedron

As White et al. (1992) and many others have observed, the spherical versions of the five platonic solids (Figure 2) represent the only ways in which the sphere can be partitioned into cells, each consisting of the same regular spherical polygon, with

the same number of polygons meeting at each vertex. The platonic solids have thus been commonly used to construct Geodesic DGGSs, although other regular polyhedra have sometimes been employed. Among these the truncated icosahedron has proved to be popular (White et al. 1992). It should be noted, however, that an equivalently partitioned DGGS could be constructed using the icosahedron itself. The other regular polyhedra remain unexplored for DGGS construction, so we limit our discussion here to the platonic solids.

In general, platonic solids with smaller faces reduce the distortion introduced when transforming between a face of the polyhedron and the corresponding spherical surface (White et al. 1998). The tetrahedron and cube have the largest face size and are thus relatively poor base approximations for the sphere. But because the faces of the cube can be easily subdivided into square quadtrees, it was chosen as the base platonic solid by Alborzi and Samet (2000). The icosahedron has the smallest face size and, therefore, any DGGSs defined on it tend to display relatively small distortions. The icosahedron is thus the most common choice for a base platonic solid. Geodesic DGGSs based on the icosahedron include those of Williamson (1968), Sadournay et al. (1968), Baumgardner and Frederickson (1985), Sahr and White (1998), White et al. (1998), Fekete and Treinish (1990), Thuburn (1997), White (2000), Song et al. (2002), and (with an adjustment as discussed in the next section) Heikes and Randall (1995a, 1995b).

Dutton chose the octahedron as the base polyhedron for the Global Elevation Model (1984) and for the Quaternary Triangular Mesh (QTM) system (1999), while Goodchild and Yang (1992) based a similar system on it, and White (2000) used it as an alternative base solid. The octahedron has the advantage that it can be oriented with vertices at the north and south poles, and at the intersection of the prime meridian and the equator,

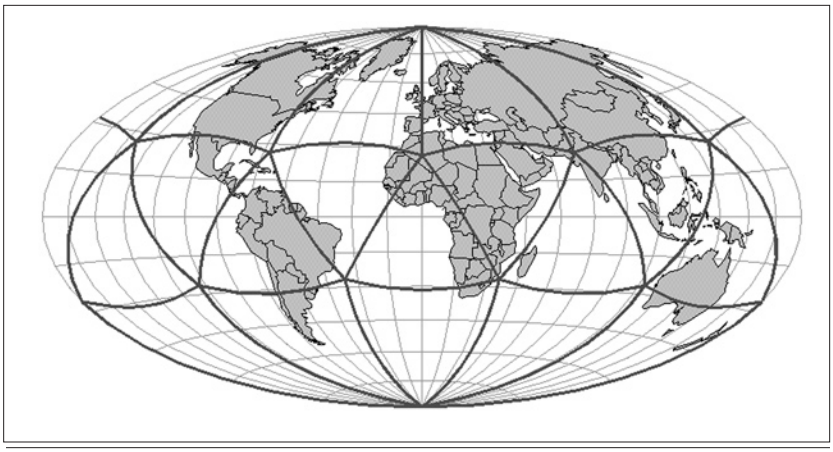

Figure 3a. Spherical icosahedron (in Mollweide projection) oriented with vertices at poles and an edge aligned with the prime meridian. Note the lack of symmetry about the equator.

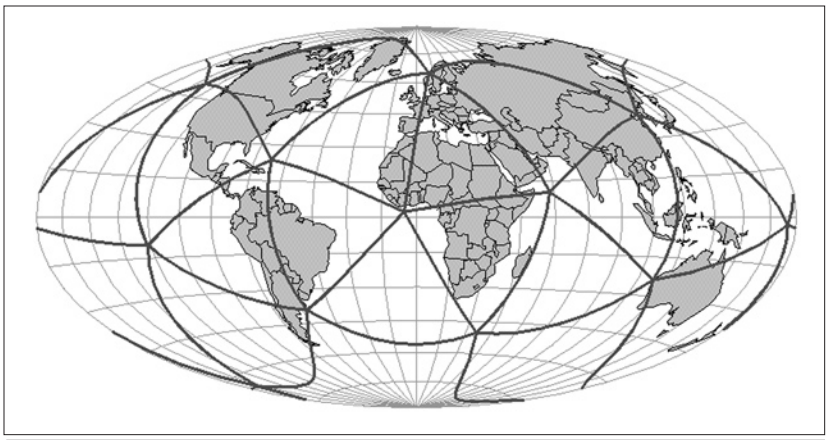

Figure 3b. Spherical icosahedron (in Mollweide projection) oriented using Fuller's Dymaxion orientation. Note that all vertices fall in the ocean.

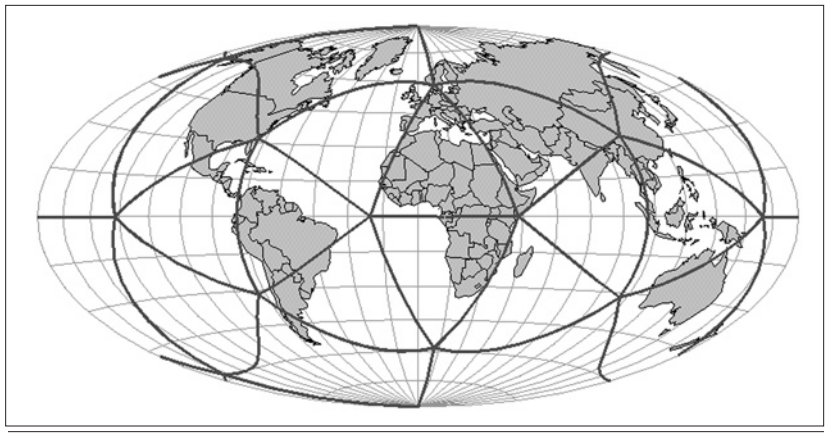

Figure 3c. Spherical icosahedron (in Mollweide projection) oriented for symmetry about equator by placing poles at edge midpoints. Note the symmetry about the equator and the single vertex falling on land.

aligning its eight faces with the spherical octants formed by the equator and prime meridian. Given a point in geographic coordinates, it is then trivial to determine on which octahedron face the point lies, but, because the octahedron has larger faces than the icosahedron, projections defined on the faces of the octahedron tend to have higher distortion (White et al. 1998).

Wickman et al. (1974) observe that if a point is placed in the center of each of the faces of a dodecahedron and then raised perpendicularly out to the surface of a circumscribed sphere ("stellated"), each of the 12 pentagonal faces becomes 5 isosceles triangles. The stellated dodecahedron thus has 60 triangular faces compared to the 20 faces of the icosahedron, and an equal area projection can be defined on the smaller faces of the stellated dodecahedron with lower distortion than on the icosahedron (e.g., Snyder 1992). However, the triangular faces are no longer equilateral and therefore such a projection displays inconsistencies along the edges between faces.

Polyhedron Orientation

Once a base polyhedron is chosen, a fixed orientation relative to the actual surface of the Earth must be specified. Alborzi and Samet (2000) oriented the cube by placing face centers at the north and south poles. White et al. (1992) oriented the truncated icosahedron such that a hexagonal face covered the continental United States. Dutton (1984, 1999), and Goodchild and Yang (1992) oriented the octahedron so that its faces align with the octants formed by the equator and prime meridian. Wickman et al. (1974) oriented the dodecahedron by placing the center of a face at the north pole and a vertex of that face on the prime meridian, thus aligning with the prime meridian an edge of one of the triangles created by stellating the dodecahedron.

In the case of the icosahedron, the most common orientation (Figure 3a) is to place a vertex at each of the poles and then align one of the edges emanating from the vertex at the north pole with the prime meridian. This orientation is used by Williamson (1968), Sadournay et al. (1968), Fekete and Treinish (1990), and Thuburn (1997).

Heikes and Randall's (1995a,b) icosahedron-based system was developed specifically for performing global climate change simulations. They note that in the common vertices-at-poles icosahedron placement (Figure 3a) the icosahedron is not symmetrical about the equator. When a simulation on a DGGS with this orientation is initialized to a state symmetrical about the equator, and then allowed to run, it evolves into a state that is asymmetrical about the equator, presumably due to the asymmetry in the underlying icosahedron. To counter this effect they rotate the southern hemisphere of the icosahedron by 36 degrees, and the resulting "twisted icosahedron" is symmetrical about the equator.

Fuller (1975) chose an icosahedron orientation (Figure 3b) for his Dymaxion icosahedral map projection that places all 12 of the icosahedron vertices in the ocean so that the icosahedron can be unfolded onto the plane without ruptures in any landmass. This is the only known icosahedron orientation with this property. Note that one compact way of specifying the orientation of a platonic solid is by giving the geographic coordinates of one of the polyhedron's vertices and the azimuth from that vertex to an adjacent vertex. For platonic solids this information will completely specify the position of all the other vertices. Using this form of specification, Fuller's Dymaxion orientation can be constructed by placing one vertex at 5.2454^0W longitude, 2.3009^0N latitude and an adjacent one at an azimuth of 7.46658^0 from the first vertex.

We note that if the icosahedron is oriented so that the north and south poles lie on the midpoints of edges rather than at vertices, then it is symmetrical about the equator without further adjustment. While maintaining this property we can minimize the number of icosahedron vertices that fall on land, following Fuller's lead. The minimal case appears to be an orientation (Figure 3c) that has only one vertex on land, in China's Sichuan Province. This orientation can be constructed by placing one vertex at 11.25^0E longitude, 58.28252^0N latitude and an adjacent one at an azimuth of 0.0^0 from the first vertex.

Spatial Partitioning Method

Once we have a base regular polyhedron, we must next choose a method of subdividing this polyhedron to create multiple resolution discrete grids. In the case of platonic solids one can define the subdivision methodology on a single face of the polyhedron or on a set of faces that constitute a unit that tiles the polyhedron, provided that the subdivision is symmetrical with respect to the face or tiling unit. Four partition topologies have been used: squares, triangles, diamonds, and hexagons.

Alborzi and Samet (2000) performed an aperture 4 subdivision to create a traditional square quadtree on each of the square faces of the cube. We have observed that the preferred choices for base platonic solid[s] are the icosahedron, the octahedron, and the stellated dodecahedron, each of which has a triangular face. The obvious choice for a triangle is to subdivide it into smaller triangles. Like the square, an equilateral triangle can be divided into n^2 (for

any positive integer n) smaller equilateral triangles by breaking each edge into n pieces and connecting the break points with lines parallel to the triangle edges (Figure 4). In geodesic dome literature this is referred to as a *Class I* or *alternate* subdivision (Kenner 1976). Recursively subdividing the triangles thus obtained generates a congruent and aligned DGGS with aperture n^2.

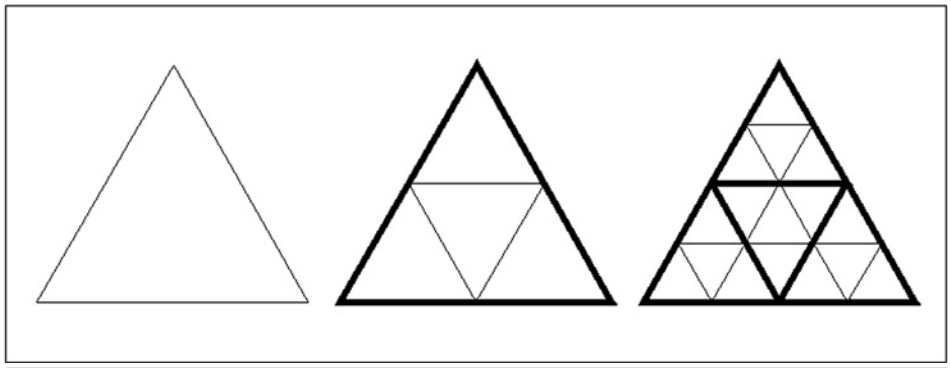

Figure 4. Three levels of a Class I aperture 4 triangle hierarchy defined on a single triangle face.

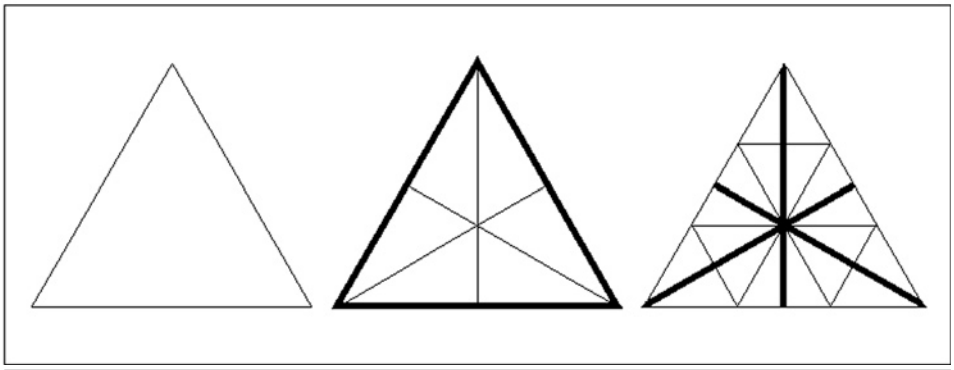

Figure 5. Three levels of a Class II aperture 3 triangle hierarchy defined on a single triangle face.

Small apertures have the advantage of generating more grid resolutions, thus giving applications more resolutions from which to choose. For congruent triangle subdivision the smallest possible aperture is 4 ($n = 2$). This aperture also conveniently parallels the fourfold recursive subdivision of the square grid quadtree; many of the algorithms developed on the square grid quadtree are transferable to the triangle grid quadtree with only minor modifications (Fekete and Treinish 1990; Dutton 1999). This subdivision approach (Figure 4) was used by Wickman et al. (1974), Baumgardner and Frederickson (1985), Goodchild and Yang (1992), Dutton (1999), Fekete and Treinish (1990), White et al. (1998), and Song et al. (2002). Congruent and unaligned Class I aperture 9 ($n = 3$) triangle hierarchies have been proposed by White et al. (1998) and Song et al. (2002).

An aperture 3 triangle subdivision is also possible. In this approach, referred to as the *Class II* or *triacon* subdivision (Kenner 1976), each triangle edge is broken into $n = 2^m$ pieces (where m is a positive integer). Lines are then drawn perpendicular to the triangle edges to form the new triangle grid (Figure 5). The Class II breakdown is incongruent and unaligned. No Geodesic DGGSs have been proposed based on this partition, though the vertices of a Class II breakdown have been used as cell points by Dutton (1984) and by Williamson (1968) to construct a dual hexagon grid.

Triangles have a number of disadvantages as the basis for a DGGS. First, they are not squares; they are thus a foreign alternative for many potential users, and they do not display as efficiently as squares on common output display devices that are based on square lattices of pixels. Like square grids, they do not exhibit uniform adjacency, each cell having three edge and nine vertex neighbors. Unlike squares, the cells of triangle-based discrete grids do not have uniform orientation; as can be seen in Figures 4 and 5, some triangles point up while others point down, and many algorithms defined on triangle grids must take into account triangle orientation.

While the square is the most popular cell region shape for planar discrete grids, its geometry makes it unusable on the triangle-faced regular polyhedra that we have seen are preferred for constructing Geodesic DGGSs. However, White (2000) notes that pairs of adjacent triangle faces may be combined to form a diamond or rhombus, and this diamond may be recursively sub-divided in a fashion analogous to the square quadtree subdivision (Figure 6). When one begins with either the octahedron or icosahedron, this yields a congruent, unaligned Geodesic DGGS with aperture 4. Because diamond-based grids have a topology identical to square-based quadtree grids they can take direct advantage of the wealth

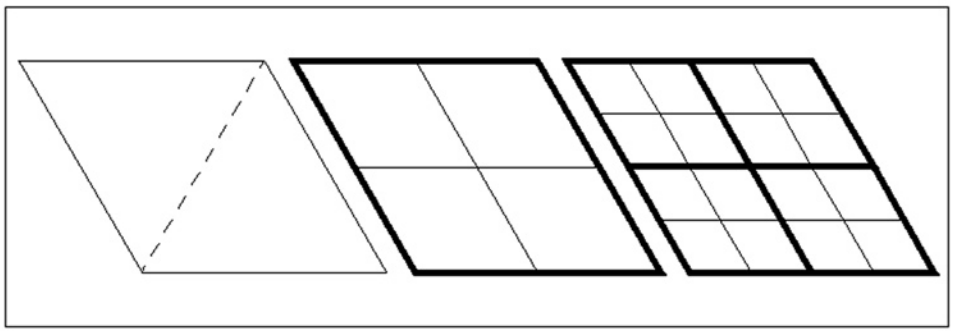

Figure 6. Three levels of an aperture 4 diamond hierarchy. The coarsest diamond resolution consists of two triangle faces as indicated.

of quadtree-based algorithms. But like square grids, they do not display uniform adjacency.

The hexagon has received a great deal of recent interest as a basis for planar discrete grids. Among the three regular polygons that tile the plane (triangles, squares, and hexagons), hexagons are the most compact, they quantize the plane with the smallest average error (Conway and Sloane 1988), and they provide the greatest angular resolution (Golay 1969). Unlike square and triangle grids, hexagon grids do have uniform adjacency; each hexagon cell has six neighbors, all of which share an edge with it, and all of which have centers exactly the same distance away from its center. Each hexagon cell has no neighbors with which it shares only a vertex. This fact alone has made hexagons increasingly popular as bases for discrete spatial simulations. Frisch et al. (1986) argue that the six discrete velocity vectors of the hexagonal lattice are necessary and sufficient to simulate continuous, isotropic, fluid flow. A recent textbook (Rothman and Zaleski 1997) on fluid flow cellular automata is based entirely on hexagonal meshes, with discussions of square meshes included "only for pedagogical calculations." Triangle grids, which are even more insufficient for this purpose, are not mentioned.

Studies by GIS researchers (Kimerling et al. 1999) and mathematicians (Saff and Kuijlaars 1997) indicate that many of the advantages of planar hexagon grids may carry over into hexagon-based Geodesic DGGSs. A hexagon-based grid has been adopted by the U.S. EPA for global sampling problems (White et al. 1992). And hexagon-based Geodesic DGGSs have been proposed at least four times in the atmospheric modeling literature (Williamson 1968; Sadournay et al. 1968; Heikes and Randall 1995a, 1995b; Thuburn 1997)—to our knowledge more often than any other Geodesic DGGS topology. It should be noted that it is impossible to completely tile a sphere with hexagons. When a base polyhedron is tiled with hexagon-subdivided triangle faces, a non-hexagon polygon will be formed at each of the polyhedron's vertices. The number of such polygons, corresponding to the number of polyhedron vertices, will remain constant regardless of grid resolution. In the case of an octahedron these polygons will be eight squares, in the case of the icosahedron they will be 12 pentagons.

While single-resolution, hexagon-based discrete grids are becoming increasingly popular, the use of multi-resolution, hexagon-based discrete grid systems has been hampered by the fact that congruent discrete grid systems cannot be built using hexagons; it is impossible to exactly decompose a hexagon into smaller hexagons (or, conversely, to aggregate small hexagons to form a larger one). Hexagons can be aggregated in groups of seven to form coarser-resolution objects which are almost hexagons (Figure 7), and these can again be aggregated into pseudo-hexagons of even coarser resolution, and so on. Known as Generalized Balanced Ternary (Gibson and Lucas 1982), this structure has become the most widely used planar multi-resolution, hexagon-based grid system. However, it has several problems as a general-purpose basis for spatial data structures. The first is that the cells are hexagons only at the finest resolution. Secondly, the finest resolution grid must be determined prior to creating the system, and once determined it is impossible to extend the system to finer resolution grids. Thirdly, the orientation of the tessellation rotates by about 19 degrees at each level of resolution. Finally, it does not appear to be possible to symmetrically tile triangular faces with such a hierarchy, which makes it unusable as a subdivision choice for a Geodesic DGGS.

There are, however, an infinite series of apertures that produce regular hierarchies of incongruent, aligned hexagon discrete grids. It should be noted that, as these hierarchies are incongruent, they do not naturally induce hierarchical data structures which are trees, and thus common tree-based algorithms cannot be directly adapted for use on these hexagon hierarchies. But it should also be noted that, as indicated previously, traditional multi-resolution vector data structures such as the geographic coordinate system are also incongruent and aligned. This may indicate that hexagon grids are more appropriate for vector applications than congruent, unaligned triangle and diamond hierarchies.

Aperture 4 is the most common choice for hexagon-based DGGSs. Figures 8 and 9 illustrate aperture 4 hexagon subdivisions corresponding to the Class I and Class II symmetry axes, respectively. The DGGSs of Heikes and Randall (1995a) and Thuburn (1997) are Class I aperture 4 hexagon grids, while Williamson (1968) uses a Class II aperture 4 hexagon grid.

As noted above, small apertures have the advantage of allowing more potential grid choices. Aperture 3 is the smallest aperture that yields an aligned hexagon hierarchy (Figure 10). In aperture 3 hierarchies the orientation of hexagon grids alternates in successive resolutions between Class I and Class II. Aperture 3 hexagon Geodesic DGGS have been proposed by a number of researchers, including Sahr and White (1998).

White et al. (1992) proposed hexagon grids of aperture 3, 4, or 7, and White et al. (1998) discussed hexagon grids of aperture 4 (Class I) and 9 (Class II). Sadournay et al. (1968) used a Class I hexagon grid of arbitrary aperture, which is incongruent and unaligned. We refer to this approach as an *n-frequency hierarchy*. Note that it is possible to construct incongruent, unaligned *n*-frequency hierarchies using triangles and diamonds as well, though, to our knowledge, this has not been proposed.

Figure 11 illustrates the most common partitioning methods defined on an icosahedron and projected to the sphere using the inverse Icosahedral Snyder Equal Area (ISEA) Projection (Snyder 1992).

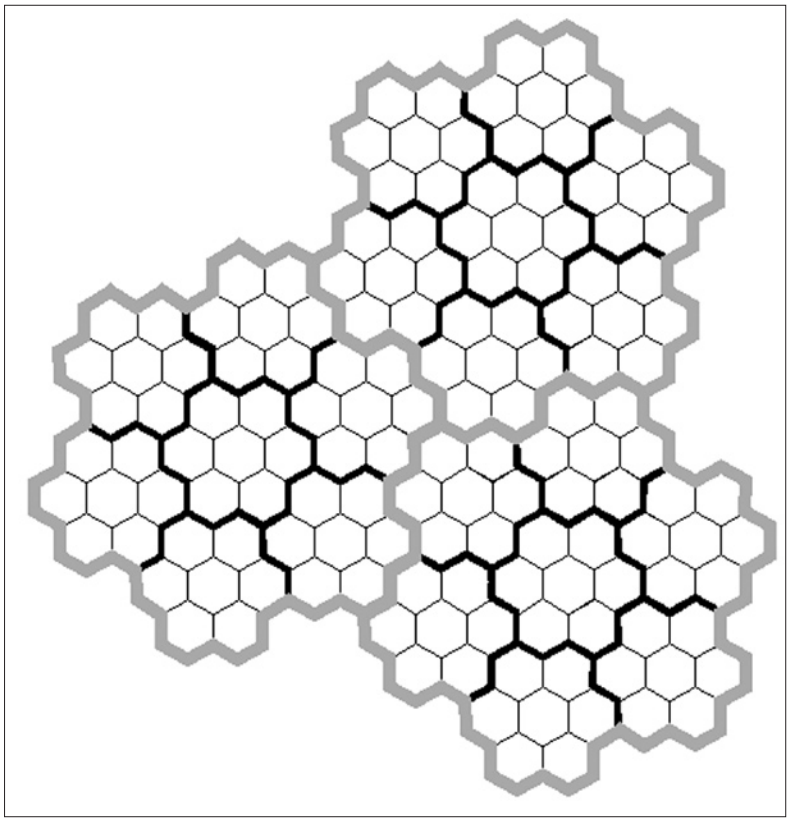

Figure 7. Seven-fold hexagon aggregation into coarser pseudo-hexagons.

Transformation

Once a partitioning method has been specified on a face or faces of the base polyhedron, a transformation must be chosen for creating a similar topology on the corresponding spherical or ellipsoidal surface. There are two basic types of approaches (Kimerling et al. 1999). *Direct spherical subdivision* approaches involve creating a partition directly on the spherical/ellipsoidal surface that maps to the corresponding partition on the planar face(s). *Map projection* approaches use an inverse map projection to transform a partition defined on the planar face(s) to the sphere/ellipsoid. White et al. (1998) provide a comparison of the area and shape distortion that occurs under a number of different transformation choices.

Perhaps the simplest approach is to perform the desired partition directly on the spherical surface, using great circle arcs corresponding to the cell edges on the planar face(s). The aperture 4 Class I triangle subdivision can be performed on the sphere by connecting the midpoints of the edges of the base spherical triangle and then, recursively performing the same operation on each of the resulting triangles. This technique was used by Baumgardner and Frederickson (1985) and Fekete and Treinish (1990). Dutton (1984) performed a Class II triangle subdivision on the surface of the octahedron and then adjusted the vertices to reflect the point elevations.

While this straightforward approach works for creating an aperture 4 triangle subdivision, it is important to note that, in general, sets of great circle arcs corresponding to the edges of planar triangle partitions do not intersect in points on the surface of the sphere, as they do on the plane. More complicated methods are needed to form spherical partitions analogous to some of the other planar partitions we have discussed.

Williamson (1968) used great circle arcs corresponding to two of the three sets of Class II triangle subdivision grid lines to determine a set of triangle vertices and then formed the last set of grid lines by connecting the existing vertices with great circle

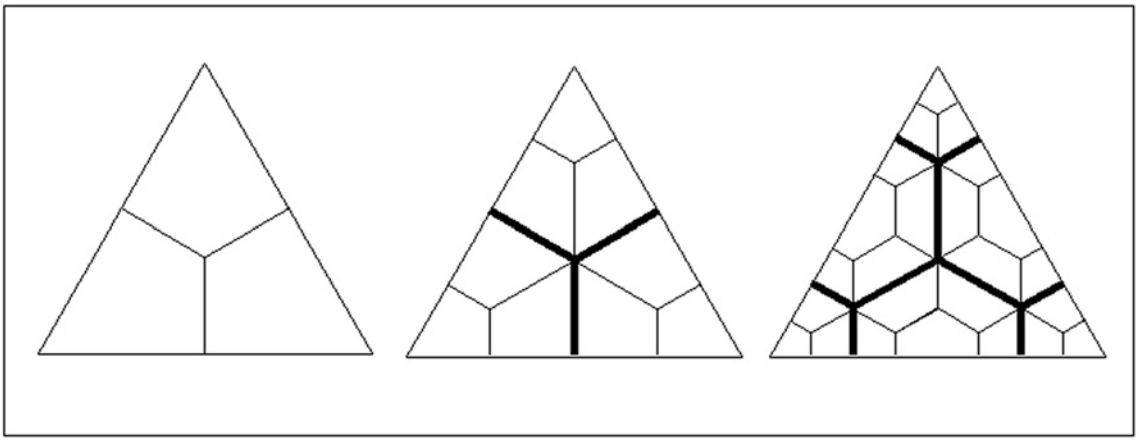

Figure 8. Three levels of a Class I aperture 4 hexagon hierarchy defined on a single triangle face.

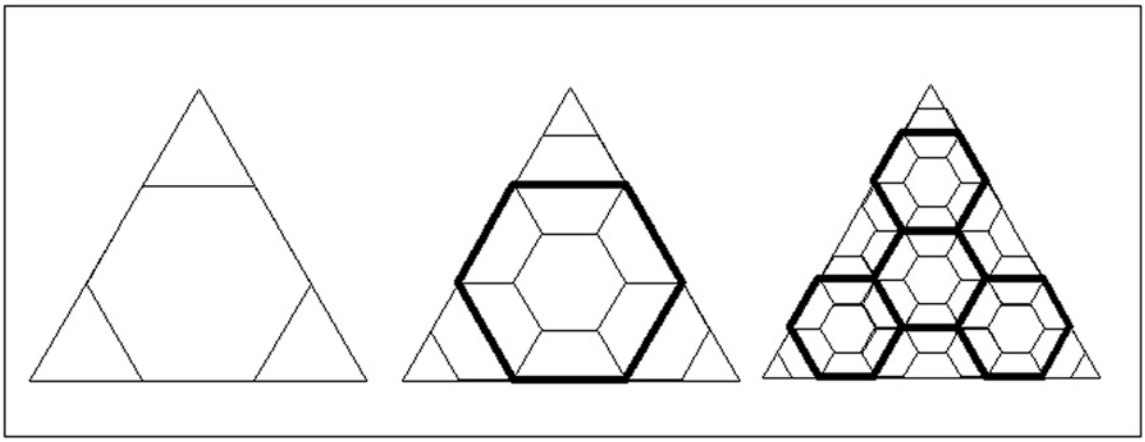

Figure 9. Three levels of a Class II aperture 4 hexagon hierarchy defined on a single triangle face.

arcs. These triangle vertices form the center points of the dual Class II aperture 4 hexagon grid (the cell edges of which are not explicitly defined).

Sadournay et al. (1968) created an aperture m (where $m = n^2$ for some positive integer n) Class I triangle subdivision on the sphere by breaking each edge of the base spherical triangle into n segments and connecting the breakpoints of two of the edges with great circle arcs. These arcs are then subdivided evenly into segments corresponding to the planar subdivision. The resulting breakpoints form the centers of the dual Class I hexagon grid. Thuburn (1997) performed a Class I aperture 4 triangle subdivision and then calculated the spherical Voronoi cells of the triangle vertices to define the dual Class I aperture 4 hexagon grid.

A number of researchers have attempted to adjust the grids created using great circle arcs to meet application-specific criteria. For instance, for many applications it would be desirable for the cell regions of each discrete grid resolution to be equal in area; the grids discussed above do not have this property. Wickman et al. (1974) began by connecting the midpoints of the base spherical triangle to form the first resolution of a Class I aperture 4 triangle grid. They then broke each of the new edges at the midpoint into two great circle arcs and adjusted the position of the breakpoint to achieve equal area quasi-triangles. This procedure is then applied recursively to yield an equal-area DGGS. Rather than using great circle arcs for triangle subdivision, Song et al. (2002) proposed using small circle arcs optimized to achieve equal cell region areas.

Heikes and Randall (1995a) constructed a Class I aperture 4 hexagon grid by taking the spherical Voronoi of the vertices of a Class I aperture 4 triangle subdivision on their twisted icosahedron. They then adjusted the grid using an optimization scheme to improve its finite difference properties for use in global climate modeling.

White et al. (1998) evaluated a number of methods for constructing triangle subdivisions on spherical triangles and observed that using appropriate inverse map projections to transform a subdivided planar triangle onto a spherical triangle may be more efficient than using recursively defined procedures. Any

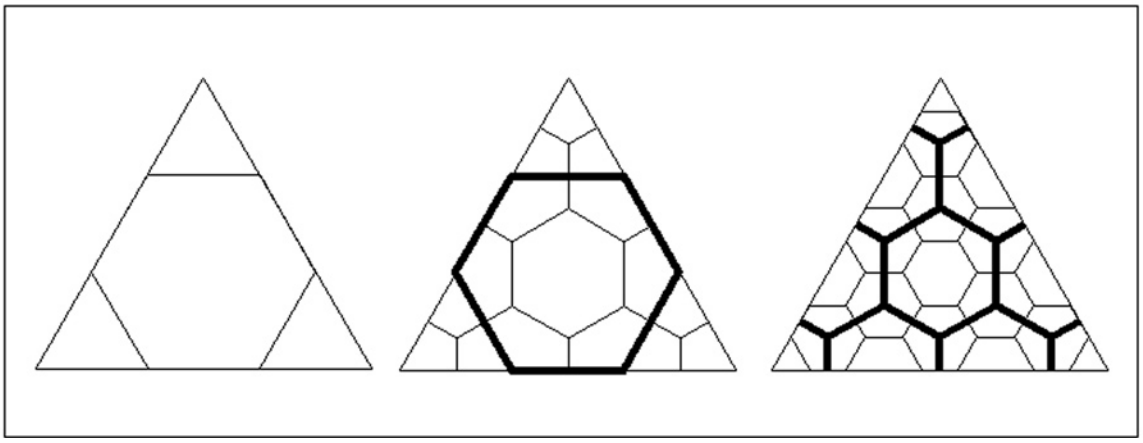

Figure 10. Three levels of an aperture 3 hexagon hierarchy defined on a single triangle face. Note the alternation of hexagon orientation (Class II, Class I, Class II, etc.) with successive resolutions.

projection may be used, provided that it maps the straight-line planar face edges to the great-circle arc edges of the corresponding spherical face.

There are at least four projections with this property. The common gnomonic projection has this property for all polyhedra but exhibits relatively large area and shape distortion. Snyder (1992) developed equal area projections defined on all of the platonic solids, but with greater shape distortion and more irregular spherical cell edges than the equal-area method of Song et al. (2002). On the icosahedron, the implementation of Fuller's Dymaxion map projection (Fuller 1975) given in Gray (1995) also has the required property but with less area and shape distortion than the gnomonic projection and less shape distortion than Snyder's icosahedral projection, though the Fuller/Gray projection is not equal area. Goodchild and Yang (1992) used a Plate Carree projection to project the faces of the octahedron to the sphere, and Dutton (1999) developed the Zenithial OrthoTriangular (ZOT) projection for the same purpose.

White et al. (1998) constructed Class I aperture 4 and 9 triangle grids on planar icosahedral faces. They also constructed a Class I aperture 4 hexagon grid by taking the dual of the aperture 4 triangle grid and a Class II aperture 9 hexagon grid by aggregating the cells of the aperture 9 triangle grid. In all cases they transformed the resulting cells to the sphere, using direct spherical subdivision or the inverse gnomonic, Fuller/Gray, or Icosahedral Snyder Equal Area (ISEA) map projections.

White et al. (1992) and Alborzi and Samet (2000) used the inverse Lambert Azimuthal Equal Area projection to project the faces of the truncated icosahedron and cube to the sphere. White et al. (1992) noted, however, that this projection does not map the straight-line planar face edges to the corresponding great-circle arc edges and, therefore, does not create a true Geodesic DGGS.

Assigning Points to Grid Cells

When specified, the points associated with grid cells are usually chosen to be the center points of the cell regions. If an inverse map projection approach is used to transform the cells from the planar faces to the sphere, then it is often convenient to choose the center points of the planar cell regions (which do not, in general, correspond to the cell region centroids on the Earth's surface) so that the points form a regular lattice, at least on patches of the plane. If the cells are formed by direct spherical subdivision, the choice of points may be complicated by the counter-intuitive behavior of great-circle arcs described above. Gregory (1999) discussed several alternatives for point selection in the case of direct spherical subdivision. Dutton's (1984) GEM DGGS used points that are the vertices of a Class II triangle subdivision. As described in the previous sub-section, the hexagonal DGGSs of Williamson (1968), Sadournay et al. (1968), Heikes and Randall (1995a), and Thuburn (1997) all specify cell center points as the vertices of a dual spherical triangle grid. The hexagonal grid cell boundaries, when specified, are created by calculating the associated spherical Voronoi cells.

Summary and Conclusions

Table 1 summarizes the design choices that define each of the Geodesic DGGSs we have discussed. Note that the number of options employed to construct a Geodesic DGGS is actually rather small, and certain choices clearly predominate in the

Reference	Base Polyhedron	Orientation	Partition	Transformation	Point Assignment
Alborzi & Samet 2000	Cube	Poles on face centers	Aperture 4 Square	Lambert Azimuthal Equal Area	Not Specified
Baumgardner & Frederickson 1985	Icosahedron	Unspecified	Aperture 4 Triangle (Class I)	Direct Spherical Subdivision	Not Specified
Dutton 1984	Octahedron	Octant aligned	Implied Aperture 3 Hexagon	Direct Spherical Subdivision	Class II Triangle Vertices
Dutton 1999	Octahedron	Octant aligned	Aperture 4 Triangle (Class I)	ZOT	Not Specified
Fekete & Treinish 1990	Icosahedron	Vertices at poles	Aperture 4 Triangle (Class I)	Direct Spherical Subdivision	Not Specified
Goodchild & Yang 1992	Octahedron	Octant aligned	Aperture 4 Triangle (Class I)	Plate Carree	Not Specified
Heikes & Randall 1995a & 1995b	Twisted Icosahedron	Vertices at poles	Twisted Aperture 4 Hexagon (Class I)	Optimized Direct Spherical Subdivision	Twisted Class I Aperture 4 Triangle Vertices
Sadourny et al. 1968	Icosahedron	Vertices at poles	*n*-frequency Hexagon (Class I)	Direct Spherical Subdivision	*n*-frequency Class I Triangle Vertices
Sahr & White 1998	Icosahedron	Equator symmetric	Aperture 3 Hexagon	ISEA	Cell Centers in ISEA Projection Space
Song et al. 2002	Icosahedron	Unspecified	Class I Aperture 4 or 9 Triangle	Equal Area Small Circle Subdivision	Not Specified
Thuburn 1997	Icosahedron	Vertices at poles	Aperture 4 Hexagon (Class I)	Direct Spherical Subdivision	Class I Aperture 4 Triangle Vertices
White et al. 1992	Truncated Icosahedron	Hexagon face covering CONUS	Aperture 3, 4, or 7 Hexagon	Lambert Azimuthal Equal Area	Not Specified
White et al. 1998	Icosahedron	Not Specified	Class I Aperture 4 or 9 Triangle or Class I Aperture 4 or Class II Aperture 9 Hexagon	Direct Spherical Subdivision, Gnomonic, ISEA, or Fuller/Gray	Not Specified
White 2000	Icosahedron or Octahedron	Not Specified	Aperture 4 Diamond	Not Specified	Not Specified
Wickman et al. 1974	Stellated Dodecahedron	Stellation vertex on pole	Aperture 4 Triangle (Class I)	Area-adjusted Direct Spherical Subdivision	Not Specified
Williamson 1968	Icosahedron	Vertices or Face Centers at Poles	Implied Class II Aperture 4 Hexagon	Direct Spherical Subdivision	Modified Class II Triangle Vertices

Table 1. Summary of Geodesic DGGS design choices.

existing designs. In particular, the icosahedron is clearly the popular choice for a base polyhedron; it is used in 10 of the 16 listed grid designs. Methods based on direct spherical subdivision are employed by about half of the grid designs. Also popular are equal area transformations, which are used by six of the grids. The grid designs are almost evenly split between triangle and hexagon partitions, but the diamond partition is a recent design that may yet prove popular due to its direct relationship to the square quadtree.

We have shown that a Geodesic DGGS can be specified through a very small number of design choices, each of which is relatively independent of the others. In effect, future Geodesic DGGS designers may pick-and-choose from the menu of design choices to construct a DGGS to meet their specific application needs. As an example, let us take each of the design decisions in turn and attempt to construct a good general-purpose Geodesic DGGS.

First, due to its lower distortion characteristics we choose the icosahedron for our base platonic solid. We orient it with the north and south poles lying on edge midpoints, such that the resulting DGGS will be symmetrical about the equator. Next we select a suitable partition. The hexagon partition has numerous advantages, and we choose aperture 3, the smallest possible aligned hexagon aperture. Because equal-area cells are advantageous for many applications, we choose the inverse ISEA projection to transform the hexagon grid to the sphere, and we specify that each DGGS point lies at the center of the corresponding planar cell region. We call the resulting grid the ISEA Aperture 3 Hexagonal (ISEA3H) DGGS. Figure 12 shows the ETOPO5 global elevation data set (Hastings and Dunbar 1998) binned into four resolutions of the ISEA3H DGGS. The elevation value

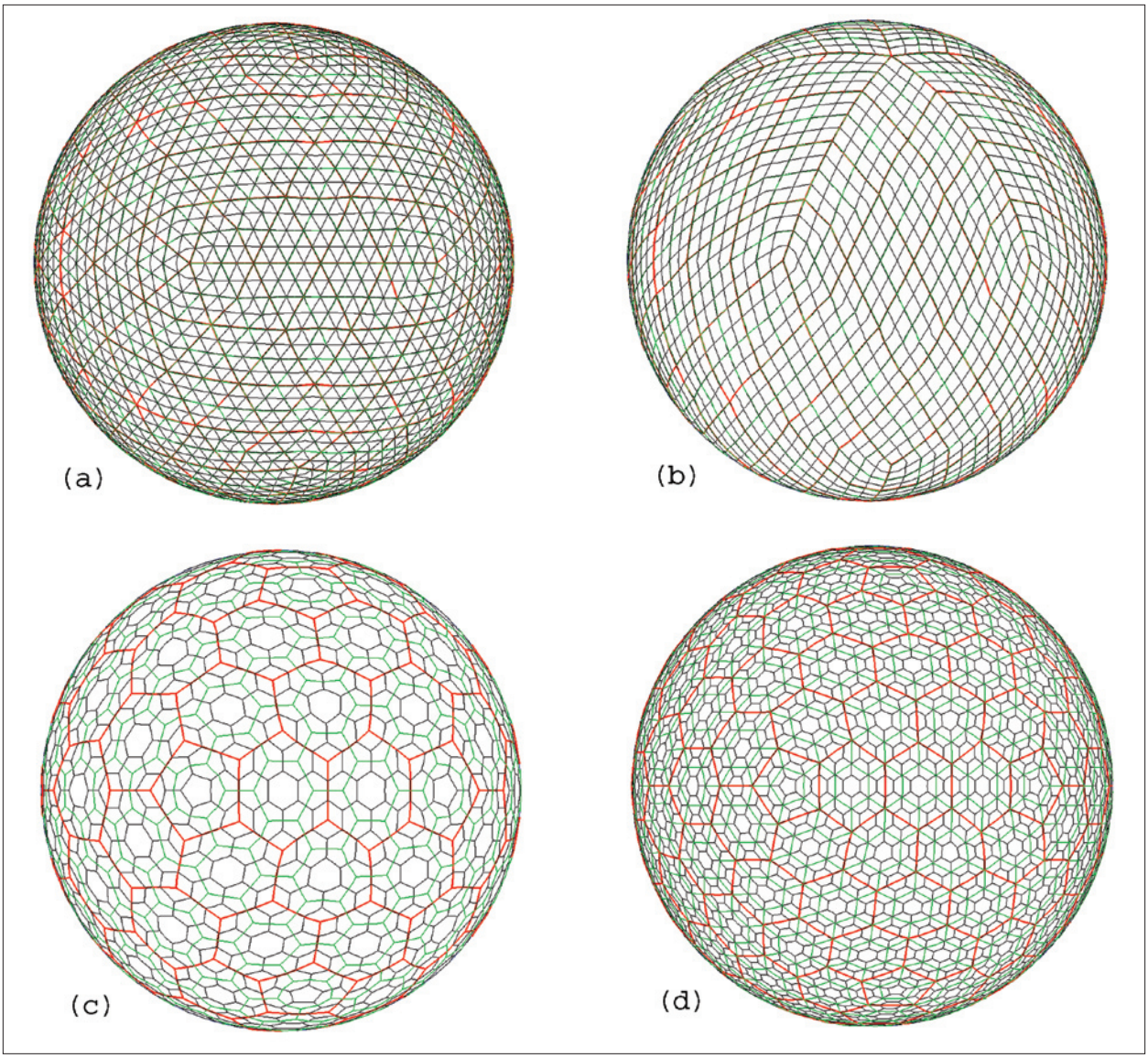

Figure 11. Three resolutions of icosahedron-based Geodesic DGGS's using four partition methods: (a) Class I aperture 4 triangle, (b) aperture 4 diamond, (c) aperture 3 hexagon, and (d) Class I aperture 4 hexagon.

for each ISEA3H cell was calculated by taking the arithmetic mean of all ETOPO5 data points that fall into that cell region. More information on this and other ISEA-based Geodesic DGGSs may be found at http://www.sou.edu/cs/sahr/dgg.

Directions for Further Research

While such studies as White et al. (1998), Kimerling et al. (1999), Clarke (2002), and the current work have made significant steps in defining and evaluating existing DGGS alternatives there remain a number of areas that we believe require further research. First, it should be noted that additional research may reveal new design choice alternatives that are superior to those already proposed. In particular, we feel that further research into transformations for Geodesic DGGS definition is required. For example, a DGGS projection that is equal area, but has less shape distortion than the ISEA projection, would be very desirable. Additionally, the grids discussed here are defined with reference to the sphere; many applications will require more accurate definitions referenced to ellipsoids. And as specific grids are chosen for practical use efficient transformations must be defined that will allow data to be moved between grids while preserving data quality.

Existing studies have treated DGGSs from the perspective of the broader GIS community, but effective evaluation of design alternatives can only take place in the context of specific applications and end-user

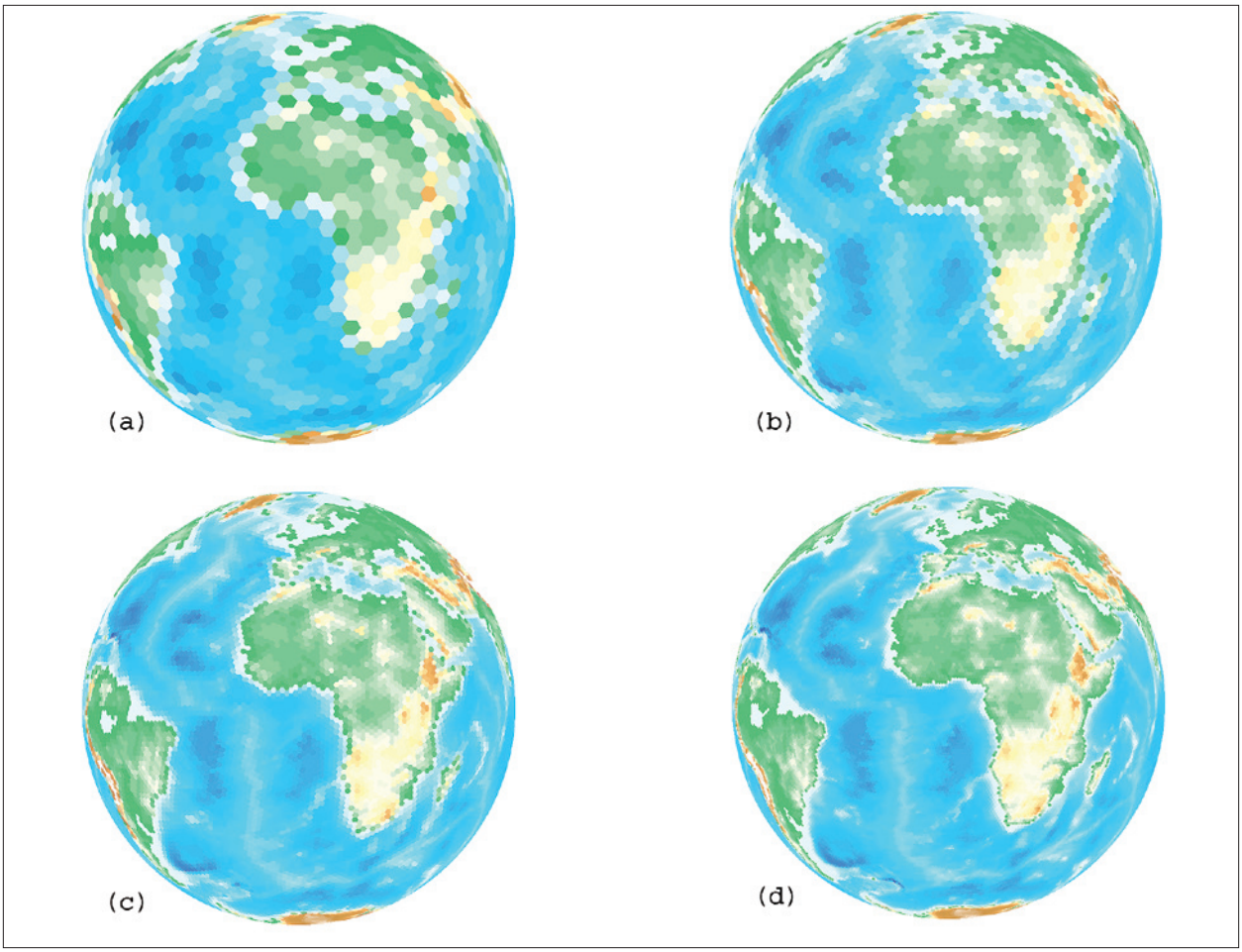

Figure 12. ETOPO5 5′ global elevation data binned into the ISEA3H Geodesic DGGS at four resolutions with approximate hexagon areas of: (a) 210,000 km^2, (b) 70,000 km^2, (c) 23,000 km^2, and (d) 7,800 km^2.

communities. In particular, the computer data structures community has yet to play a significant role in DGGS evaluation. Input from this community, which should play a key role in making appropriate design choices in the future, has been primarily limited to the adaptation of quadtree algorithms to aperture 4 triangle grids (in particular the QTM DGGS of Dutton (1999)). Hexagon-based Geodesic DGGSs, which have clear advantages for many end-users, remain largely ignored. A significant effort must be made by the data structures community to develop and evaluate algorithms for the regular, but non-tree, hierarchies they form.

ACKNOWLEDGEMENTS

Portions of this research were sponsored by the USDA Forest Service under cooperative agreement PNW-92-0283, and by the U.S. Environmental Protection Agency (EPA) under cooperative agreement CR821672 and contract 1B0250NATA. The research has not been subjected to the EPA's peer and administrative review and, hence, does not necessarily reflect the views of the Agency.

REFERENCES

Alborzi, H., and H. Samet. 2000. Augmenting SAND with a spherical data model. Paper presented at the First International Conference on Discrete Global Grids. Santa Barbara, California, March 26-28.

Bailey, H.P. 1956. Two grid systems that divide the entire surface of the Earth into quadrilaterals of equal area. *Transactions of the American Geophysical Union* 37: 628-35.

Baumgardner, J.R., and P.O. Frederickson. 1985. Icosahedral discretization of the two-sphere. *SIAM Journal of Numerical Analysis* 22(6):1107-14.

Bell, S.B., B.M. Diaz, F. Holroyd, and M.J. Jackson. 1983. Spatially referenced methods of processing raster and vector data. *Image and Vision Computing* 1(4): 211-20.

Brooks, D.R. 1981. Grid systems for Earth radiation budget experiment applications. *NASA Technical Memorandum 83233*. 40 pp.

Chen, J., X. Zhao, and Z. Li. 2003. An algorithm for the generation of Voronoi diagrams on the sphere based on QTM. *Photogrammetric Engineering & Remote Sensing* 69(1): 79-90.

Clarke, K.C. 2002. Criteria and measures for the comparison of global geocoding systems. In: M.F. Goodchild, and A.J. Kimerling (eds), *Discrete global grids: A web book*. University of California, Santa Barbara.[http://www.ncgia.ucsb.edu/globalgrids-book].

Conway, J. H., and N. J. A. Sloane. 1998. *Sphere packings, lattices, and groups*. New York, New York: Springer-Verlag. 679p.

Dutton, G. 1984. Geodesic modelling of planetary relief. *Cartographica* 21(2&3, Monograph 32-33): 188-207.

Dutton, G. 1999. A hierarchical coordinate system for geoprocessing and cartography. Berlin, Germany: Springer-Verlag. 231p.

Fekete, G., and L. Treinish. 1990. Sphere quadtrees: A new data structure to support the visualization of spherically distributed data. *SPIE, Extracting Meaning from Complex Data: Processing, Display, Interaction* 1259: 242-50.

Frisch, U., B. Hasslacher, and Y. Pomeau, Y. 1986. Lattice-gas automata for the Navier-Stokes equations. *Physics Review Letters* 56: 1505-8.

Fuller, R. B. 1975. *Synergetics*. New York, New York: MacMillan. 876p.

Gibson, L. and D. Lucas. 1982. Spatial data processing using generalized balanced ternary. In: *Proceedings, IEEE Computer Society Conference on Pattern Recognition and Image Processing*. Las Vegas, Nevada, June 14-17. pp. 566-571.

Golay, J.E. 1969. Hexagonal parallel pattern transformations. *IEEE Transactions on Computers* C-18(8): 733-9.

Goodchild, M.F., and S. Yang. 1992. A hierarchical spatial data structure for global geographic information systems. *Graphical Models and Image Processing* 54(1): 31-44.

Gray, R. W. 1995. Exact transformation equations for Fuller's world map. *Cartographica* 32(3): 17-25.

Gregory, M. 1999. Comparing inter-cell distance and cell wall midpoint criteria for discrete global grid systems. Unpublished Masters thesis. Department of Geosciences, Oregon State University. 258p.

Hastings, D.A., and P.K. Dunbar. 1998. Development and assessment of the global one-km base elevation digital elevation model (GLOBE). *ISPRS Archives* 32(4): 218-21.

Heikes, R., and D. A. Randall. 1995a. Numerical integration of the shallow-water equations on a twisted icosahedral grid. Part I: Basic design and results of tests. *Monthly Weather Review* 123(6):1862-80.

Heikes, R., and D. A. Randall. 1995b. Numerical integration of the shallow-water equations on a twisted icosahedral grid. Part II: A detailed description of the grid and an analysis of numerical accuracy. *Monthly Weather Review* 123(6):1881-7.

Kenner, H. 1976. *Geodesic math and how to use it*. Berkeley, California: University of California Press. 172p.

Kimerling, A.J., K. Sahr, D. White, and L. Song. 1999. Comparing geometrical properties of global grids. *Cartography and Geographic Information Science* 26(4): 271-87.

Kurihara, Y. 1965. Numerical integration of the primitive equations on a spherical grid. *Monthly Weather Review* 93: 399-415.

Lukatela, H. 2002. A seamless global terrain model in the Hipparchus system. In: M.F. Goodchild, and A.J. Kimerling (eds), *Discrete global grids: A web book*. University of California, Santa Barbara. [http://www.ncgia.ucsb.edu/globalgrids-book].

Olsen, A.R., D.L. Stevens, and D. White. 1998. Application of global grids in environmental sampling. In: S. Weisberg (ed.), *Computing Science and Statistics, vol. 30: Proceedings of the 30th Symposium on the Interface, Computing Science and Statistics*. Minneapolis, Minnesota, May 13-16. Interface Foundation of North America, Fairfax Station, Virginia. pp. 279-84.

Otoo, E.J., and H. Zhu. 1993. Indexing on spherical surfaces using semi-quadcodes. In: Abel, D.J., and B.C. Ooi (eds), *Advances in spatial databases*, Proceedings of the Third International Symposium on Advances in Spatial Databases, Singapore, June 23-25. pp. 510-29.

Paul, M.K. 1973. On computation of equal area blocks. *Bulletin Geodésique* 107: 73-84.

Rothman, D.H., and S. Zaleski. 1997. *Lattice-gas cellular automata: Simple models of complex hydrodynamics*. Cambridge, U.K.: Cambridge University Press. 297p.

Sadourny, R., A. Arakawa, and Y. Mintz. 1968. Integration of the nondivergent barotropic vorticity equation with an icosahedral-hexagonal grid for the sphere. *Monthly Weather Review* 96(6): 351-6.

Saff, E.B., and A. Kuijlaars. 1997. Distributing many points on a sphere. *Mathematical Intelligencer* 19(1): 5-11.

Sahr, K., and D. White. 1998. Discrete global grid systems. In: S. Weisberg (ed.), Computing Science and Statistics (Volume 30): Proceedings of the 30th Symposium on the Interface, Computing Science and Statistics. Minneapolis, Minnesota, May 13-16. Interface Foundation of North America, Fairfax Station, Virginia. pp. 269-78.

Snyder, J. P. 1992. An equal-area map projection for polyhedral globes. *Cartographica* 29(1): 10-21.

Song, L., A. J. Kimerling, and K. Sahr. 2002. Developing an equal area global grid by small circle subdivision. In: M.F. Goodchild, and A.J. Kimerling (eds), *Discrete global grids: A web book*. University of California, Santa Barbara.[http://www.ncgia.ucsb.edu/globalgrids-book].

Stefanakis, E., and M. Kavouras. 1995. On the determination of the optimum path in space. In: Frank, A.U., and W. Kuhn (eds), *Proceedings of the 2nd International Conference on Spatial Information Theory (COSIT '95)*, Semmering, Austria, September 21-23. New York, New York: Springer. pp. 241-57.

Thuburn, J. 1997. A PV-based shallow-water model on a hexagonal-icosahedral grid. *Monthly Weather Review* 125: 2328-47.

Tobler, W.R., and Z. Chen. 1986. A quadtree for global information storage. *Geographical Analysis* 18(4): 360-71.

White, D., A. J. Kimerling, and W. S. Overton. 1992. Cartographic and geometric components of a global sampling design for environmental monitoring. *Cartography and Geographic Information Systems* 19(1): 5-22.

White, D., A. J. Kimerling, K. Sahr, and L. Song. 1998. Comparing area and shape distortion on polyhedral-based recursive partitions of the sphere. *International Journal of Geographical Information Science* 12: 805-27.

White, D. 2000. Global grids from recursive diamond subdivisions of the surface of an octahedron or icosahedron. *Environmental Monitoring and Assessment* 64(1): 93-103.

Wickman, F. E., E. Elvers, and K. Edvarson. 1974. A system of domains for global sampling problems. *Geografiska Annaler* 56(3/4): 201-12.

Williamson, D. L. 1968. Integration of the barotropic vorticity equation on a spherical geodesic grid. *Tellus* 20(4): 642-53.